Supporting Information

Metal-Organic Framework-Derived Hybrid Co_3O_4-Carbon Porous Nanowire Arrays as Reversible Oxygen Evolution Electrodes

*Tian Yi Ma,[1] Sheng Dai,[1] Mietek Jaroniec[2] and Shi Zhang Qiao[1,]**

[1] School of Chemical Engineering, The University of Adelaide, Adelaide, SA 5005, Australia.

E-mail:s.qiao@adelaide.edu.au

[2] Department of Chemistry and Biochemistry, Kent State University, Kent, Ohio 44240, USA.

1. Experimental

1.1. Material preparation

Metal-organic framework (MOF) grown on Cu foil. 0.3 mmol of dipotassium 2,6-naphthalene-dicarboxylate and 0.3 mmol of cobalt(II) acetate tetrahydrate were mixed in aqueous solution at room temperature under vigorous stirring. The solution was then transferred into a Teflon-lined stainless steel autoclave. The Cu foil repeatedly rinsed with absolute ethanol and Milli-Q water through sonication treatment was fixed with Teflon clamps and introduced into the autoclave, and immersed in the reaction solution with the unprotected side facing downwards, while the other side of Cu foil was protected against nanowire array growth by applying a nail-polish coating layer. The autoclave was sealed and maintained at 80 ºC for 20 h and then allowed to cool down to room temperature. The MOF composed of $Co(C_{12}H_6O_4)(H_2O)_4$ grown on Cu foil, was subjected to repeated washing and drying under ambient conditions overnight. The aforementioned composition was confirmed by X-ray diffraction and elemental analysis.

Hybrid Co_3O_4-carbon porous nanowire arrays grown on Cu foil (Co_3O_4C-NA). The as-synthesized Co-based MOF grown on Cu foil was transferred into a tube furnace and carbonized in flowing N_2 atmosphere. Specifically, the material was first heated from room temperature to 400 °C with a ramp rate of 1 °C min^{-1}, and the temperature was kept at 400 °C for 2 h, which was further increased to 600 °C and stabilized for another 4 h, followed by cooling down to room temperature. The resultant product, hybrid Co_3O_4-carbon porous nanowire arrays grown on Cu foil, was denoted as Co_3O_4C-NA. The loading amount of nanowire arrays on Cu foil was ~0.2 mg cm^{-2}, which was determined by using the increased mass of Cu foil. These values were roughly consistent from batch to batch using the identical synthetic procedure.

Co_3O_4 porous nanowire arrays grown on Cu foil (Co_3O_4-NA). The carbon-free counterpart of Co_3O_4C-NA was prepared by calcination of the as-synthesized Co_3O_4C-NA in air to remove carbon

species. Specifically, Co_3O_4C-NA was heated from room temperature to 500 °C with a heating rate of 1 °C min^{-1}, and the temperature was kept at 500 °C for 4 h, followed by cooling down to room temperature. The resultant product was denoted as Co_3O_4-NA.

IrO_2-carbon coated on Cu foil (IrO_2/C). The synthesis of the IrO_2-carbon composite catalyst was performed by using a slightly modified method reported by Zhao et al. (*Nat. Commun.* **2013**, *4*, 2390) and Hara et al. (*J. Phys. Chem. A* **2000,** *104*, 5275). Typically, 0.1 g of K_2IrCl_6 was added to 50 mL of aqueous solution containing 0.167 g of disodium hydrogen citrate sesquihydrate. The pH of the red-brown solution was adjusted to 7.5 with 0.25 M NaOH solution. The resulting mixture was heated to 95 °C for 30 min under constant stirring, and cooled down to room temperature. The addition of NaOH solution at room temperature followed by heating at 95 °C for 30 min was repeated until its pH value was stabilized at a level of 7.5. Next, the solution was transferred to a round-bottom flask with a reflux condenser followed by dispersion of 0.05 g of carbon powder (Vulcan XC-72). The mixture was kept at 95 °C for 2 h with bubbled O_2 through the solution. After vacuum-drying at 70 °C, the sample was heated at 300 °C for 30 min to remove the organic compounds, and washed with distilled water. Finally, the sample was collected by filtration and subjected to drying at 60 °C; this catalyst contained IrO_2 supported on ~52 wt.% of carbon, which was identical to the carbon content in Co_3O_4C-NA. Next, the specified amount of the as-synthesized IrO_2-carbon composite catalyst was ultrasonically dispersed into the mixture of 1 mL Milli-Q water and 1 mL isopropanol. The dispersion was transferred onto the cleaned Cu foil via a controlled drop casting method. The mass of the IrO_2-carbon composite was controlled to obtain a loading amount of 0.2 mg cm^{-2}, the same as that of Co_3O_4C-NA on Cu foil. The resulting electrode (IrO_2/C) was subjected to overnight solvent evaporation in air, subsequent coating with a thin layer of Nafion® solution (1.0 wt.% water solution), and drying in air for another 1 h.

Physically mixed Co_3O_4 porous nanowire arrays and carbon powder coated on Cu foil. The as-synthesized Co_3O_4-NA was carefully scraped off from Cu foil, physically mixed with carbon

powder (Vulcan XC-72) by strong sonication treatment conducted in a Cell Crusher to achieve a very good dispersion and interaction between Co_3O_4-NA and carbon powder. The carbon content was controlled to be ~52 wt.%, identical to that in Co_3O_4C-NA. The obtained mixture was dispersed into the solution containing 1 mL Milli-Q water and 1 mL isopropanol, and then transferred onto the cleaned Cu foil via a controlled drop casting method to afford a loading amount of 0.2 mg cm^{-2}. The resulting electrode was subjected to overnight solvent evaporation in air, subsequent coating with a thin layer of Nafion® solution (1.0 wt.% water solution), and drying in air for another 1 h.

Porous nanowire arrays coated on glassy carbon electrodes. The as-synthesized Co_3O_4C-NA and Co_3O_4-NA were carefully scraped off from Cu foil, ultrasonically dispersed into the mixture of 1 mL Milli-Q water and 1 mL isopropanol, and then transferred onto the glassy carbon electrode via a controlled drop casting method, with a loading amount of 0.2 mg cm^{-2}. The resulting electrode was subjected to overnight solvent evaporation in air, subsequent coating with a thin layer of Nafion® solution (1.0 wt.% water solution), and drying in air for another 1 h.

1.2. Physicochemical characterization

Transmission electron microscopy (TEM) images were obtained on a Philips CM200 microscope at an acceleration voltage of 200 kV. Scanning electron microscopy (SEM) images were recorded on the FEI Quanta 450 at high vacuum with an accelerating voltage of 10 kV. X-ray diffraction (XRD) patterns were collected on a powder X-ray diffractometer at 40 kV and 15 mA using Co-Kα radiation (Miniflex, Rigaku). X-ray photoelectron spectra (XPS) were obtained using an Axis Ultra (Kratos Analytical, UK) XPS spectrometer equipped with an Al Kα source (1486.6 eV). The elemental analysis (EA) was conducted by inductively coupled plasma (ICP) emission spectroscopy on a Thermo Jarrell-Ash ICP-9000 (N + M) spectrometer, and by a WS-CHN800 elemental analyzer. Before EA, the samples were degassed under vacuum in order to eliminate interference from surface-adsorbed species. Thermogravimetric analysis (TG) was measured using a Setaram

Labsys Thermogravimetric Analyzer in air, over a range from room temperature to 800 °C with a heating rate of 10 °C min^{-1}. N_2 adsorption isotherms were collected on a Tristar II Micromeritics adsorption analyzer at the liquid nitrogen temperature (-196 °C). Pore size distributions were calculated using the adsorption branch of the isotherms by Barrett-Joyner-Halenda (BJH) method; surface areas were obtained by the Brunauer-Emmett-Teller (BET) method using adsorption data at a relative pressure range of P/P_0 = 0.05-0.30; and total pore volumes were estimated from the volume adsorbed at a relative pressure (P/P_0) of 0.994. The synthesized nanowire array materials were carefully scraped off from Cu foil and used for TEM, XRD, XPS, EA, TG and N_2 adsorption measurements, and no detectable Cu was found by these measurements. For SEM, the nanowire arrays grown on Cu foil were observed directly.

1.3. Electrochemical characterization

OER measurements were performed in a three-electrode glass cell. The data were recorded using a CHI 760 D bipotentiostat (CH Instruments, Inc., USA). The synthesized nanowire arrays grown on Cu foil were directly used as the working electrode for electrochemical characterizations. The reference electrode was Ag/AgCl in 4 M KCl solution and the counter electrode was a platinum wire. The current density was normalized to the geometrical surface area and the measured potentials *vs.* Ag/AgCl were converted to a reversible hydrogen electrode (RHE) scale according to the Nernst equation ($E_{RHE} = E_{Ag/AgCl} + 0.059 \times pH + 0.205$). A flow of O_2 was maintained over the electrolyte (0.1 M or 1.0 M KOH) during electrochemical measurements in order to ensure the O_2/H_2O equilibrium at 1.23 V *vs.* RHE. The polarization curves were recorded with the scan rate of 0.5 mV s^{-1}. The working electrodes were scanned for several times until the signals were stabilized, and then the data for polarization curves were collected, corrected for the iR contribution within the cell. The Tafel slope was calculated according to Tafel equation as follows:

$$\eta = b \cdot log(j/j_0)$$

where η denotes the overpotential, b denotes the Tafel slope, j denotes the current density, and j_0 denotes the exchange current density. The onset potentials were determined based on the beginning of the linear region in Tafel plots. The overpotential was calculated as follows:

$$\eta = E\ (vs.\ RHE) - 1.23$$

considering O_2/H_2O equilibrium at 1.23 V *vs.* RHE.

To investigate the reaction mechanism for OER, rotating ring-disk electrode (RRDE) voltammograms were conducted on a RRDE configuration (Pine Research Instrumentation, USA) consisting of a glassy carbon disk electrode and a Pt ring electrode. The synthesized hybrid porous nanowire arrays were carefully scraped off from Cu foil, ultrasonically dispersed into the mixture of water and isopropanol, and then coated onto the RRDE using nafion as the binder. A scan rate of 0.5 mV s^{-1} and a rotation rate of 1500 rpm were applied for RRDE tests. Specifically, in order to determine the reaction pathway for OER by detecting the HO_2^- formation, the ring potential was held constantly at 1.50 V *vs.* RHE for oxidizing HO_2^- intermediate in O_2-saturated 0.1 M KOH; on the other hand, to ensure that the oxidation current originates from oxygen evolution rather than other side reactions and to calculate the Faradaic efficiency of the system, the ring potential was held constantly at 0.40 V *vs.* RHE to reduce the O_2 formed from the catalyst on the disk electrode in N_2-saturated 0.1 M KOH solution. A continuous OER (disk electorde) → ORR (ring electrode) process occurred on the RRDE (**Figure S8**). The Faradaic efficiency (ε) was calculated as follows:

$$\varepsilon = I_r/(I_d N)$$

where I_d denotes the disk current, I_r denotes the ring current, and N denotes the current collection efficiency of the RRDE, which was determined using the same configuration with an IrO_2 thin-film electrode to be 0.2. To properly calculate the Faradaic efficiency of the system, the disk electrode was held at a relatively small constant current of 200 μA (~1 mA cm^{-2}); this current is sufficiently large to ensure an appreciable O_2 production and sufficiently small to minimize local saturation and bubble formation at the disk electrode (see *McCrory et al., J. Am. Chem. Soc. 2013, 135, 16977*).

IrO_2 thin-film electrode was chosen for the calibration of collection efficiency of the RRDE, because it is free of possible carbon oxidation during OER and is a well-known standard catalyst with nearly 100% Faradaic efficiency (see T. Nakagawa, et al. *J. Am. Chem. Soc.* **2009**, *131*, 15578).

Electrochemical impedance spectroscopy (EIS) measurements were performed by applying an AC voltage with 5 mV amplitude in a frequency range from 100000 to 1 Hz and recorded at 1.60 V *vs.* RHE. The electrical double layer capacitor (C_{dl}) and surface roughness factor (R_f) of the as-synthesized materials were measured from double-layer charging curves using cyclic voltammograms (CVs) in a small potential range of 1.10–1.15 V. Working electrodes were scanned for several potential cycles until the signals were stabilized, and then the CV data were collected. The plot of current density (at 1.14 V) against scan rate has a linear relationship and its slope is the double layer capacitance (C_{dl}). The R_f was calculated by dividing C_{dl} by the capacitance of ideal planar metal oxides (*e.g.* Co_3O_4) having smooth surface, normally taken to be 60 μF cm^{-2} (see L. M. da Silva, et al., Determination of the morphology factor of oxide layers, *Electrochim. Acta* **2001**, *47*, 395).

For polarization curves recorded in the whole region of ORR and OER, the experimental conditions were identical to those used in OER measurements. Specifically, the synthesized nanowire arrays grown on Cu foil were directly used as the working electrode in a three-electrode glass cell. The 0.1 M KOH electrolyte was saturated by a continuous flow of O_2 during the reaction. A scan rate of 0.5 mV s^{-1} was applied, and the working electrodes were scanned for several times until stabilization before the polarization curves were recorded. To investigate the ORR reaction pathway, the as-synthesized Co_3O_4C-NA was carefully scraped off from Cu foil, ultrasonically dispersed in the mixture of water and isopropanol, and then coated onto the RRDE using nafion as the binder. The RRDE voltammograms were recorded at the constant ring potential (1.50 V *vs.* RHE) suitable for oxidizing possible HO_2^- intermediate using scan rate of 0.5 mV s^{-1} and rotation rate of

1500 rpm in O_2-saturated 0.1 M KOH. The electron transfer number (n) and HO_2^- intermediate production percentage (% HO_2^-) were determined as follows:

$$n = 4I_d/(I_d + I_r/N)$$

$$\%HO_2^- = 200I_r/(I_dN + I_r)$$

where I_d denotes the disk current, I_r denotes the ring current, and N denotes the current collection efficiency.

2. Supplementary figures

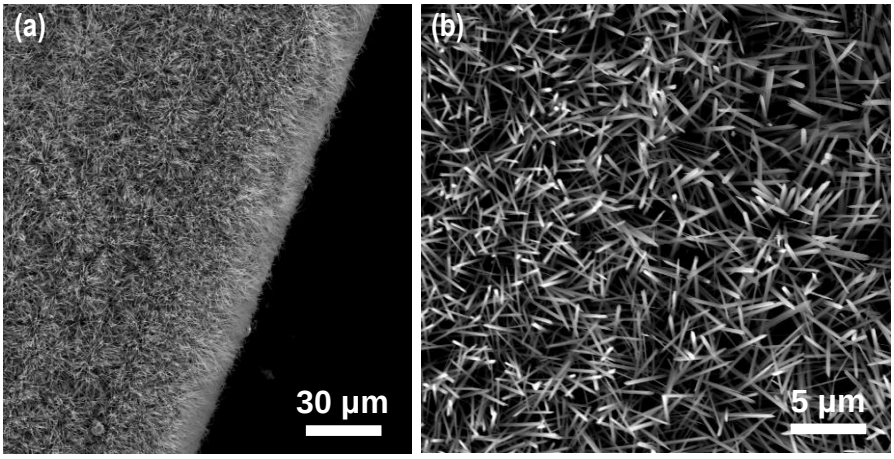

Figure S1. SEM images of the Co-based MOF grown on Cu foil.

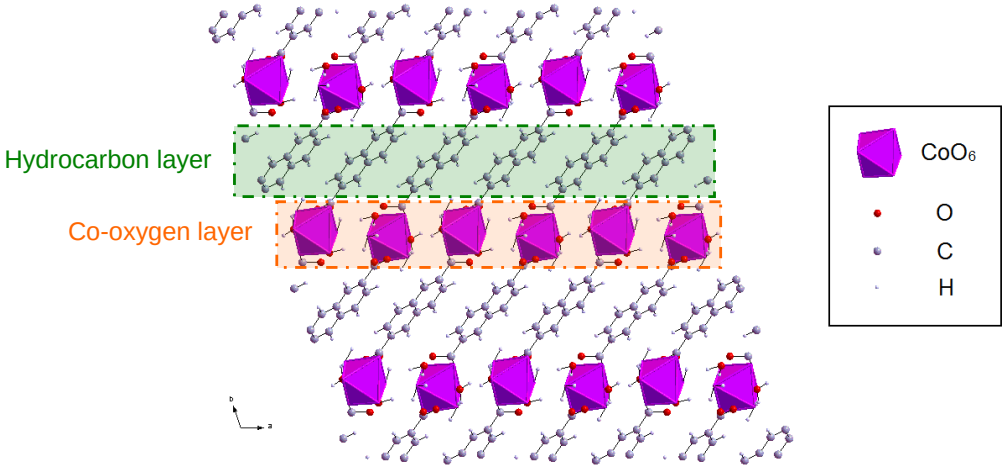

Figure S2. Crystal structure of the MOF composed of $Co(C_{12}H_6O_4)(H_2O)_4$, used as the precursor for synthesizing Co_3O_4C-NA. The MOF prepared in this work is of the same structure to that described by J. A. Kaduk (*J. Appl. Cryst.* **2001**, *34*, 710), as confirmed by XRD and elemental analysis. The $Co(C_{12}H_6O_4)(H_2O)_4$ compound crystallizes in the triclinic space group $P\bar{1}$. The Co cations are octahedrally coordinated, and each Co is coordinated to two *trans* monodentate carboxylates and four equatorial water molecules. Each naphthalenedicarboxylate bridges two Co atoms. The full crystal structure data (in CIF format) is provided as a separate supplementary file (see **CIF S1**). As shown in Figure S2, the crystal structure consists of alternating organic hydrocarbon and inorganic CoO_6 layers, in which the hydrocarbon layers can be transformed into carbon, while the CoO_6 layers can be transformed into Co_3O_4 nanocrystals through carbonization in N_2. Also, the deterioration and carbonization upon heat treatment of this layered structure prefers to form slit-like pores (see J. K. Sun, et al. Q. *Energy Environ. Sci.* **2014**, *7*, 2071), which agrees well with TEM and N_2 adsorption results (Figures 1c and 2b in the main text).

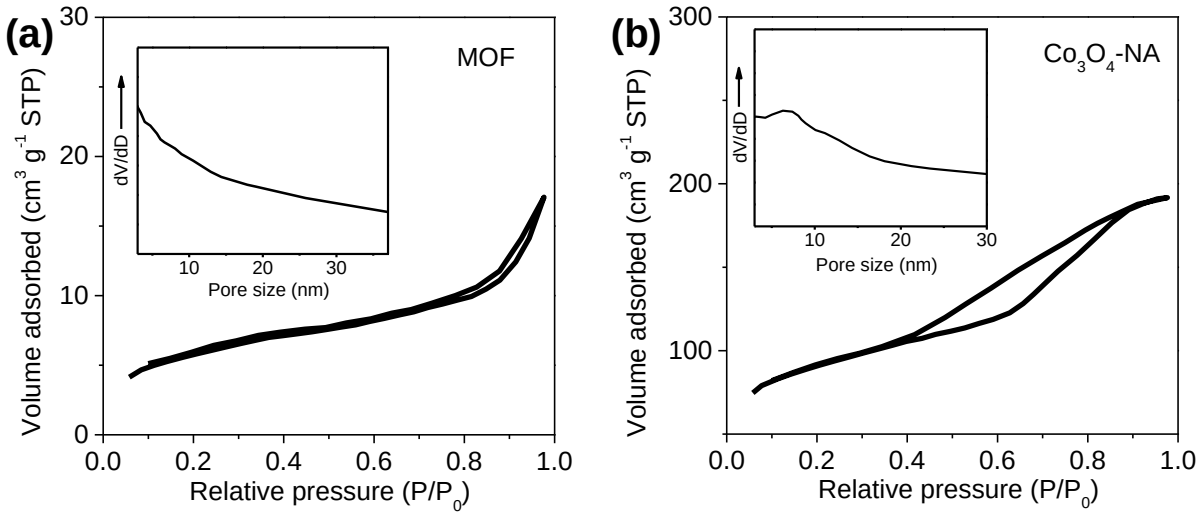

Figure S3. N_2 adsorption isotherms recorded for (a) the Co-based MOF (without evacuation of the coordinated solvent molecules in the MOF crystals) and (b) Co_3O_4-NA, and the corresponding pore size distribution curves for (inset in panel a) the MOF and (inset in panel b) Co_3O_4-NA. The surface areas of the MOF and Co_3O_4-NA were determined to be 25 and 283 m^2 g^{-1}, respectively. The low surface area of the $Co(C_{12}H_6O_4)(H_2O)_4$ MOF is probably due to its dense layered crystalline structure without open-framework pores, as well as the extensively existing coordinated H_2O in the MOF crystals before solvent molecule evacuation.

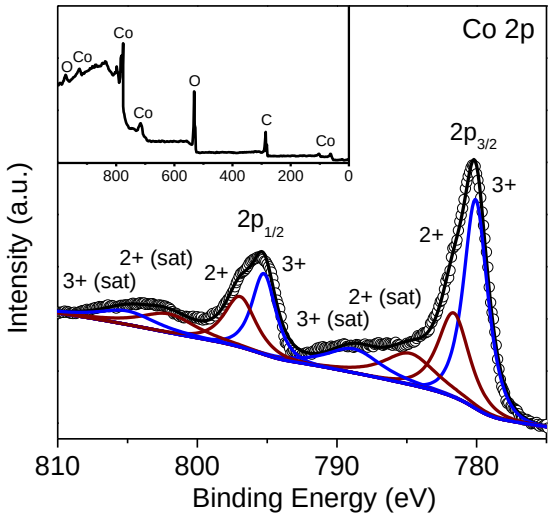

Figure S4. High resolution XPS spectrum of Co 2p core level and (inset) XPS survey spectrum of Co_3O_4-NA.

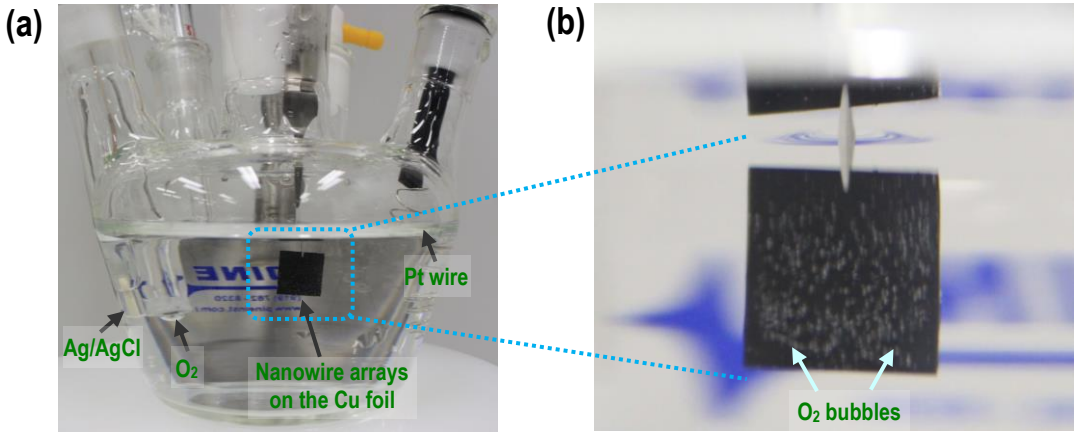

Figure S5. Optical image of electrocatalytic OER process, showing (a) the three-electrode glass cell and (b) bubbles on the surface of Co_3O_4C-NA that was directly used as the working electrode (operating at 1.70 V *vs.* RHE in 0.1 M KOH), indicating the formation of O_2.

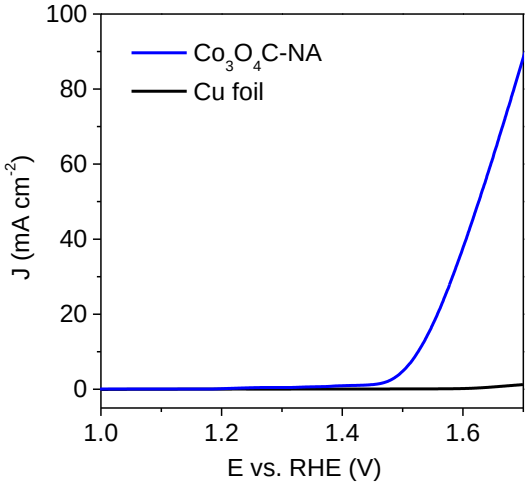

Figure S6. Polarization curves of Cu foil and Co_3O_4C-NA, showing negligible activity of Cu foil in comparison to that of Co_3O_4C-NA.

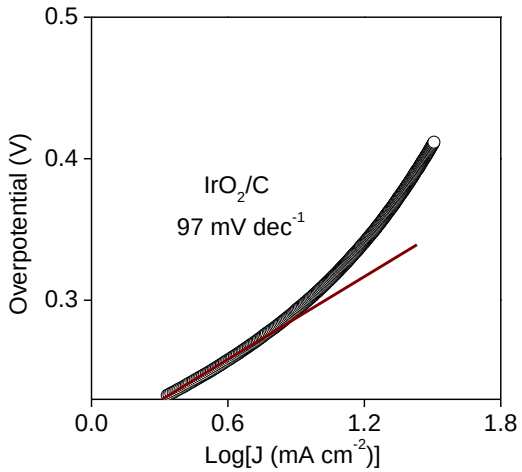

Figure S7. Tafel plot of IrO_2/C with a slope value of 97 mV decade^{-1}.

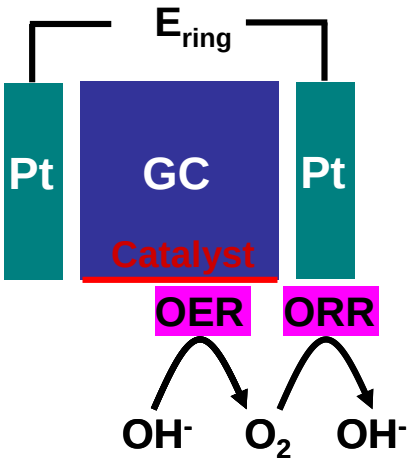

Figure S8. Schematic illustration of the continuous OER (disk eletrode) → ORR (ring electrode) process initiated on a RRDE.

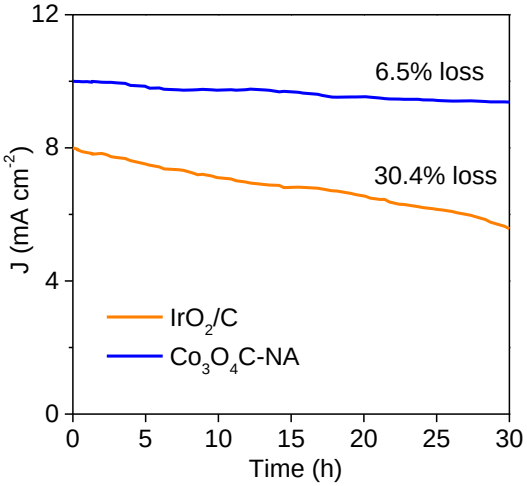

Figure S9. Chronoamperometric response of Co_3O_4C-NA and IrO_2/C at a constant potential of 1.52 V.

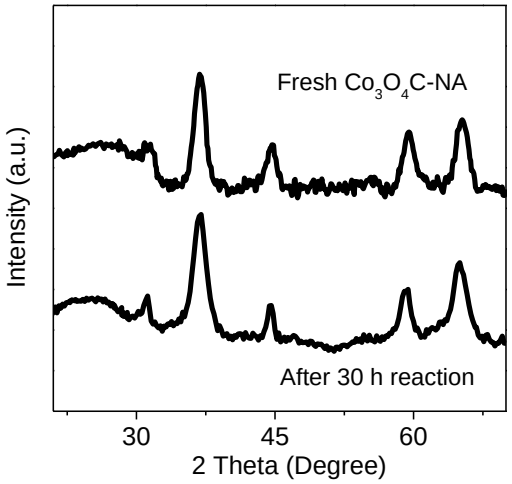

Figure S10. XRD patterns of Co_3O_4C-NA and the catalyst after 30 h reaction at a constant potential of 1.52 V.

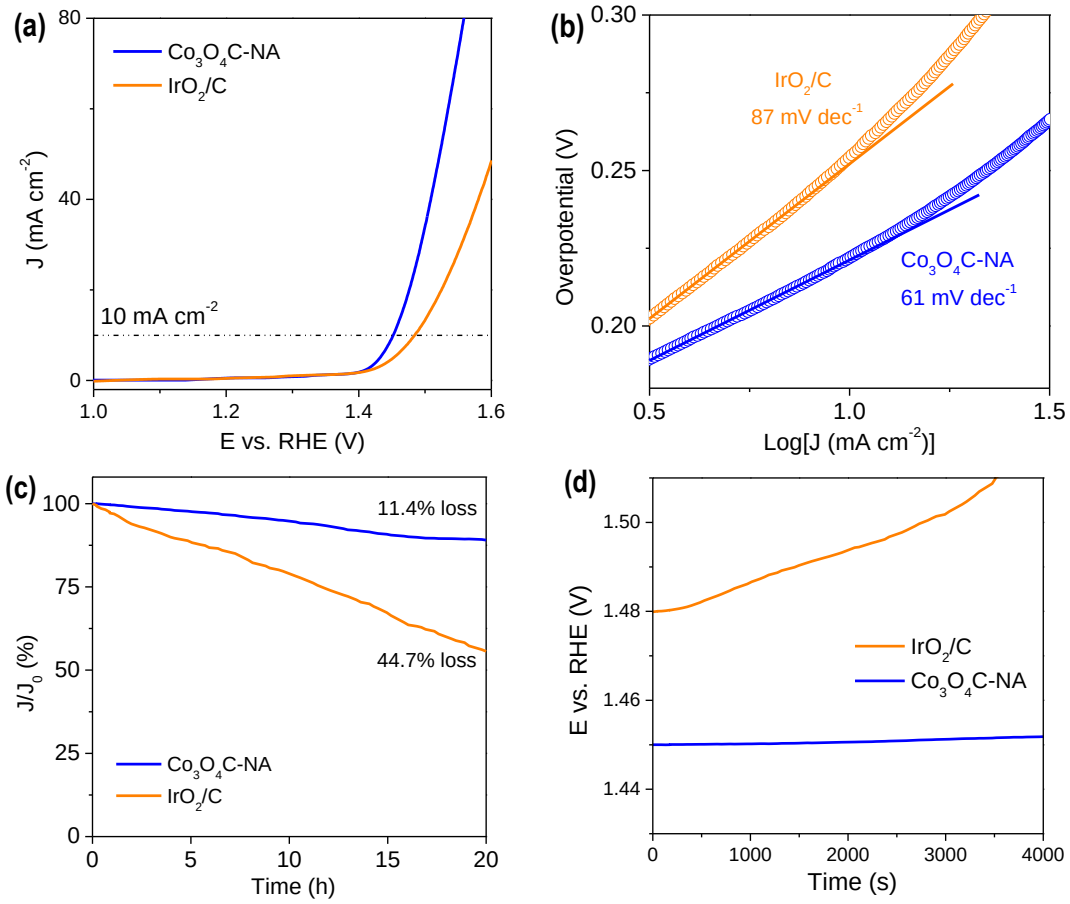

Figure S11. (a) Polarization curves and (b) Tafel plots of Co_3O_4C-NA and IrO_2/C in an O_2-saturated 1.0 M KOH solution (scan rate: 0.5 mV s^{-1}). (c) Chronoamperometric response at a constant potential of 1.45 V recorded for Co_3O_4C-NA and IrO_2/C. (d) Chronopotentiometric response at a constant current density of 10.0 mA cm^{-2} recorded for Co_3O_4C-NA and IrO_2/C. The smooth performance of catalysts in concentrated alkaline solutions is critical for real applications. Thus, we further tested the OER activity and stability of the as-synthesized catalysts in 1.0 M KOH solution. The high activity of Co_3O_4C-NA is well preserved with a sharp onset potential at 1.41 V, and it can deliver a current density of 10.0 mA cm^{-2} at 1.45 V, which is much lower than that of IrO_2/C at 1.48 V (Figure S11a). The Tafel slope value of Co_3O_4C-NA (61 mV $decade^{-1}$) is lower than that of IrO_2/C (87 mV $decade^{-1}$, Figure S11b), suggesting better catalytic activity with more favorable reaction kinetics of Co_3O_4C-NA. The chronoamperometric response of Co_3O_4C-NA shows an anodic current attenuation of 11.4% within 20 hours, much samller than that of IrO_2/C (44.7%, Figure S11c); also, the chronopotentiometric response of Co_3O_4C-NA indicates its operating potential stable at 1.45 V to deliver a 10.0 mA cm^{-2} current density, whereas the operating potential of IrO_2/C increases obviously within 4000 s (Figure S11d). These facts demonstrate much stronger durability of active materials directly grown on Cu foil than that of the post-coated catalysts on electrodes.

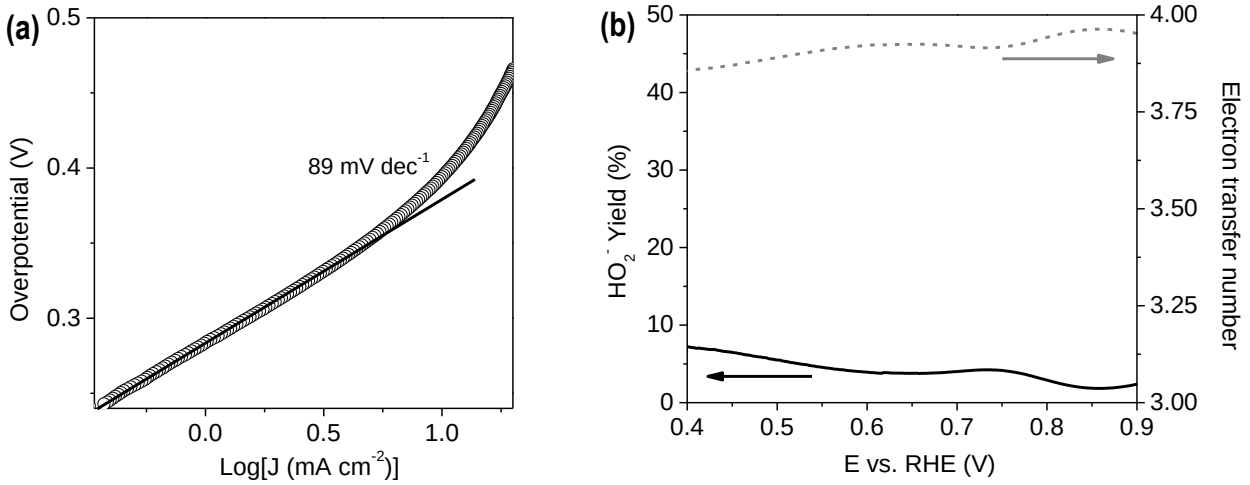

Figure S12. (a) Tafel plot of Co_3O_4C-NA in the ORR region, affording a slope value of 89 mV decade^{-1}. The Co_3O_4C-NA grown on Cu foil was directly used as the working electrode for ORR. (b) Extent of HO_2^- production and the corresponding electron-transfer number based on RRDE measurements. The Co_3O_4C-NA was scraped off from Cu foil and coated on the RRDE (see details in Experimental Section). An electron transfer number of 3.85−3.96 was confirmed in the potential range of 0.40 to 0.90 V, showing the four-electron ORR pathway with few peroxide intermediates.

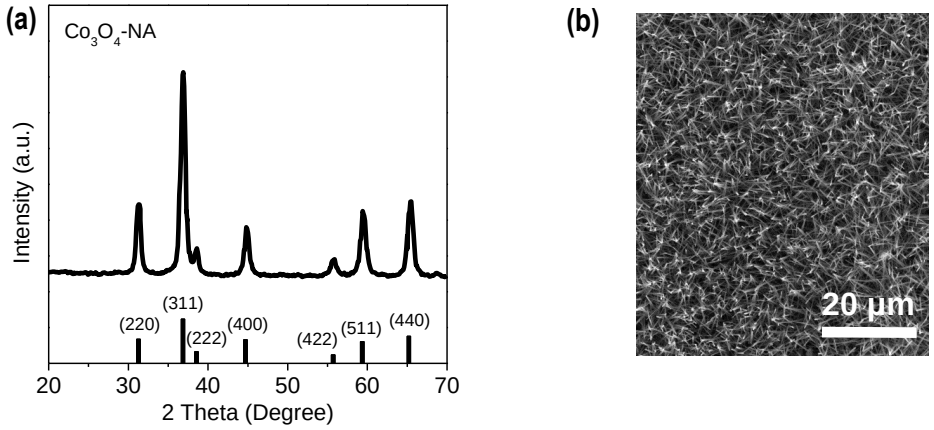

Figure S13. (a) XRD pattern and (b) SEM image of Co_3O_4-NA, indicating pure cubic spinel-phase Co_3O_4 with the nanowire array morphology.

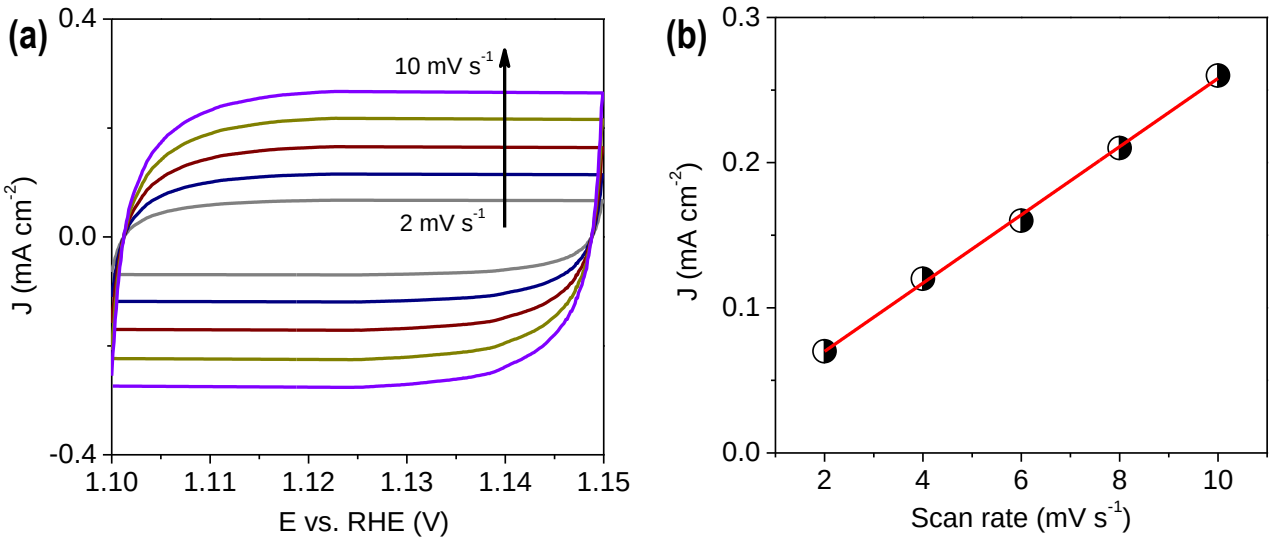

Figure S14. (a) CVs of IrO_2/C coated on Cu foil measured in 0.1 M KOH at scan rates of 2 to 10 mV s^{-1}. (b) A plot of the current density at 1.14 V *vs.* the scan rate to determine the double layer capacitance (C_{dl}) and the roughness factor (R_f). The C_{dl} and R_f values of the as-synthesized electrocatalysts were evaluated on the basis of CVs. The CVs of IrO_2/C supported on Cu foil were recorded at different scan rates (2–10 mV s^{-1}) in a potential region of 1.10–1.15 V (ΔE = 50 mV). The CVs exhibit an approximate rectangular shape of an electrical double layer capacitor (Figure S14a). In this potential region, charge transfer electrode reactions are considered to be negligible and the current is originated solely from electrical double layer charging and discharging. The plot of current density (at 1.14 V) against potential scan rate has a linear relationship (Figure S14b), and its slope is the double layer capacitance (C_{dl} of IrO_2/C: 22.3 mF cm^{-2}). The surface roughness factor, R_f, was calculated to be 371 for IrO_2/C, by dividing the electrode capacitance by 60 μF cm^{-2} (see details in Experimental Section).

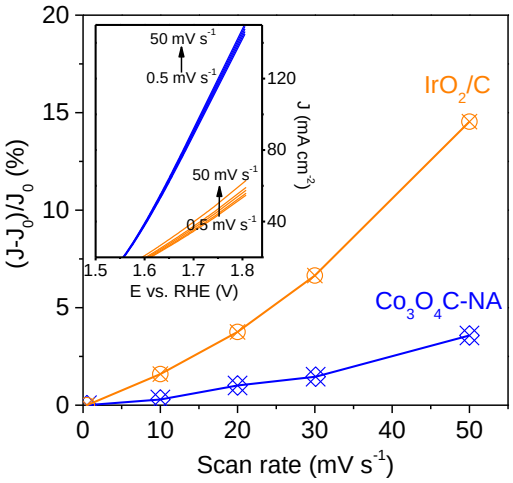

Figure S15. The current density (recorded at 1.80 V in the polarization curve, originated from OER) increased percentage *vs.* the scan rate of Co_3O_4C-NA and IrO_2/C. (Inset) Polarization curves of Co_3O_4C-NA and IrO_2/C at different scan rates in the range of 0.5 to 50 mV s^{-1}. The working electrodes were scanned for several times until the signals were stabilized, and then the polarization curves were collected.

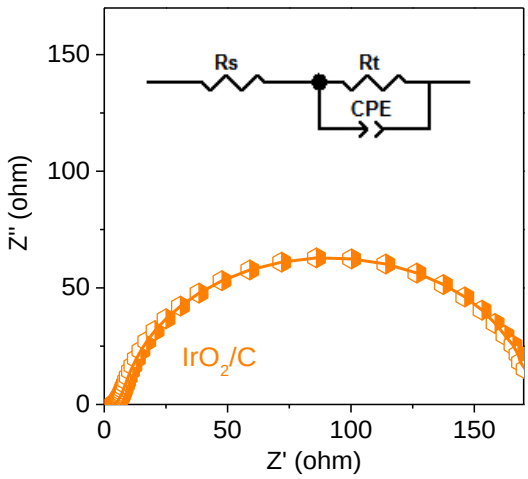

Figure S16. EIS of IrO_2/C coated on Cu foil recorded at 1.60 V with inset showing the corresponding equivalent circuit diagram, consisting of an electrolyte resistance (Rs), a charge-transfer resistance (Rt) and a constant-phase element (CPE).

3. Supplementary table

Table S1. Comparison of the OER activity for several recently reported highly active transition-/noble-metal and non-metal catalysts supported on different substrates.

Catalyst	*Potential @ 10.0 mA cm^{-2} (V vs. RHE)*	*Tafel slope (mV dec^{-1})*	*Mass loading (mg cm^{-2})*	*Electrolyte*	*Substrate*	*Reference*
Co_3O_4C-NA	1.52	70	~0.2	0.1 M KOH	Cu foil	This work
N-doped graphene-CoO	1.57	71	0.7	1.0 M KOH	Glassy carbon	[S1]
Co_3O_4/N-doped-graphene	1.54	67	1.0	1.0 M KOH	Ni foam	[S2]
Mn_3O_4/$CoSe_2$	1.68	49	0.2	0.1 M KOH	Glassy carbon	[S3]
$Zn_xCo_{3-x}O_4$ nanowire array	1.55	51	~1.0	1.0 M KOH	Ti foil	[S4]
$Ni_xCo_{3-x}O_4$ nanowire array	~1.60	59–64	2.3–2.7	1.0 M NaOH	Ti foil	[S5]
Ni-substituted Co_3O_4 nanowire array	~1.60	65–74	N.A.	1.0 M NaOH	Ni foam	[S6]
IrO_2/C	1.60	N.A.	0.2	0.1 M KOH	Glassy carbon	[S7]
Rutile RuO_2	>1.70	N.A.	0.05	0.1 M KOH	Glassy carbon	[S8]
$Ru_{0.2}Ir_{0.8}O_2$	1.62	N.A.	0.38	0.5 M H_2SO_4	Gold substrate	[S9]
g-C_3N_4-CNT composite	1.60	83	0.2	0.1 M KOH	Glassy carbon	[S10]
N-doped graphene-CNT composite	>1.70	141	N.A.	0.1 M KOH	Self-supported membrane	[S11]
N-doped graphitic carbon	1.61	75–80	0.2	0.1 M KOH	Glassy carbon	[S7]

References:

[**S1**] S. Mao, Z. Wen, T. Huang, Y. Hou, J. Chen, *Energy Environ. Sci.* **2014**, *7*, 609–616.

[**S2**] Y. Liang, Y. G. Li, H. L. Wang, J. G. Zhou, J. Wang, T. Regier, H. J. Dai, *Nat. Mater.* **2011**, *10*, 780−786.

[**S3**] M. R. Gao, Y. F. Xu, J. Jiang, Y. R. Zheng, S. H. Yu, *J. Am. Chem. Soc.* **2012**, *134*, 2930–2933.

[**S4**] X. Liu, Z. Chang, L. Luo, T. Xu, X. Lei, J. Liu, X. Sun, *Chem. Mater.* **2014**, *26*, 1889–1895.

[**S5**] Y. Li, P. Hasin, Y. Wu, *Adv. Mater.* **2010**, *22*, 1926–1929.

[**S6**] B. Lu, D. Cao, P. Wang, G. Wang, Y. Gao, *Int. J. Hydrogen Energy* **2011**, *36*, 72–78.

[**S7**] Y. Zhao, R. Nakamura, K. Kamiya, S. Nakanishi, K. Has himoto, *Nat. Commun.* **2013**, *4*, 2390.

[**S8**] Y. Lee, J. Suntivich, K. J. May, E. E. Perry, Y. Shao-Horn, *J. Phys. Chem. Lett.* **2012**, *3*, 399−404.

[**S9**] N. Mamaca, E. Mayousse, S. Arrii-Clacens, T. W. Napporn, K. Servat, N. Guillet, K. B. Kokoh, *Appl. Catal. B: Environ.* **2012**, *111–112*, 376–380.

[**S10**] T. Y. Ma, S. Dai, M. Jaroniec, S. Z. Qiao, *Angew. Chem. Int. Ed.* **2014**, *53*, 7281–7285.

[**S11**] S. Chen, J. J. Duan, M. Jaroniec, S. Z. Qiao, *Adv. Mater.* **2014**, *26*, 2925–2930.

4. Supplementary video

Video S1. Co_3O_4C-NA directly used as the working electrode for OER at operating potentials of 1.60 V, 1.70 V and 1.80 V *vs.* RHE.

The video indicates that the generation of O_2 gas increases at elevated operating potentials. Even at high operating potential of 1.80 V (delivering a large current density of ~140 mA cm^{-2}), no peeling of the catalysts is observed, showing the strong adhesion between hybrid porous nanowire arrays and Cu foil, and the outstanding structural stability of the synthesized oxygen electrode. Moreover, the vast majority of the generated O_2 gas is quickly and efficiently released from the surface of electrodes in the form of tiny bubbles, rather than accumulating into very large ones. This is because nanowire arrays can effectively burst the larger O_2 bubbles that often stick to the planar catalyst film surface, and wick the evolved bubbles, thus maintaining the solid-liquid interface (see D. Kong, et al. *J. Am. Chem. Soc.* **2014**, *136*, 4897; M. S. Faber, et al. *J. Am. Chem. Soc.* **2014**, *136*, 10053). This phenomenon suppresses the loss of available surface area blocked by the evolved O_2 bubbles, which may also contribute to the excellent performance of the catalyst, especially at high operating potentials.

5. Supplementary crystallographic information file (CIF)

CIF S1. The CIF file of the Co-based MOF, $Co(C_{12}H_6O_4)(H_2O)_4$, which is used as the precursor for the synthesis of Co_3O_4C-NA. This CIF data are obtained from the IUCr's electronic archives with the reference number of HN0121, which were first reported by J. A. Kaduk (*J. Appl. Cryst.* **2001**, *34*, 710),